Chapter 1

Theoretical bases

Just after the discovery of nuclear magnetic resonance (NMR) in 1945 in bulk matter [Blo46, Pur46] this phenomenon has become of interest for many structural elucidation techniques. NMR can measure a magnetic moment produced by spin charged atoms embedded to the strong magnetic field. It took 25 years from continuous wave (CW) low resolution detection techniques till development of pulse Fourier spectroscopy, which enables an expansion of modern high-resolution NMR techniques. The response to a δ-function pulse according to the superposition principle, which is valid in linear systems, is a linear superposition of the responses of all frequency components called FID (*free induction decay*) and the transfer function, called spectrum, can be obtained from the FID by a Fourier transformation. The Fourier transformation became a routine for characterization of a spectrum in modern NMR instruments. Further improvements were made with discovery of a new dimension, where frequency response spectrum $S(\omega)$ became a spectrum of two variables $S(\omega_1, \omega_2)$. The two-dimensional (2D) spectroscopy [Ern87] was able to distinguish between two independent precession periods, i.e. evolution and detection period. The evolution during preceding period is monitored indirectly through the phase and amplitude of the magnetization at the beginning of the detection period. This scheme has many crucial advantages, for example, to observe multiple quantum coherence indirectly.

In this chapter the theoretical bases of NMR will be presented in a very short overview. We will focus our interest to the solid state NMR with connection to the spin-$\frac{1}{2}$ systems. Magic angle spinning experiment for dipolar coupled spin-$\frac{1}{2}$pair will be also presented. We will conclude this chapter with the bases of 2D spectroscopy. Deep theoretical descriptions

of NMR can be found in monographs like e.g. Abragam ([Abr61]) and Ernst et al. ([Ern87]). The methods of solid state NMR spectroscopy are fully or partially described in monographs from Mehring ([Meh83]) and Slichter ([Sli92]). The possible applications on polymers are discussed in monograph from Schmidt-Rohr/Spiess ([SR94]). In this monograph, for convenience, we will assume all Hamiltonians as the operators correspond to $E/\hbar$, where energy eigenvalues are measured in angular frequency units.

1.1 Types of interactions in NMR

The dynamics of N coupled spins is not possible to describe in terms of the motion of classical magnetization vectors, but it is necessary to treat quantum mechanical formalism. The most convenient description of quantum mechanical system dynamics can be made with the help of density operator $\hat{\boldsymbol{\rho}}$. We will recall some of its basic properties

$$\hat{\boldsymbol{\rho}} = \hat{\boldsymbol{\rho}}^{+}, \qquad \mathbf{Tr}\,\{\hat{\boldsymbol{\rho}}\} = 1, \qquad \hat{\boldsymbol{\rho}}^{2} = \hat{\boldsymbol{\rho}}\,. \tag{1.1}$$

For the time-dependent Schröninger equation [Ern87, Sli92], one can derive the equation of motion for the density operator $\hat{\boldsymbol{\rho}}$ under Hamiltonian $\hat{\boldsymbol{H}}$

$$\frac{d}{dt}\,\hat{\boldsymbol{\rho}}(t) = -i[\hat{\boldsymbol{H}}(t), \hat{\boldsymbol{\rho}}(t)], \tag{1.2}$$

called Liouville-von Neumann equation or simply density operator equation. Its formal solution may be written

$$\hat{\boldsymbol{\rho}}(t) = \hat{\boldsymbol{U}}(t)\,\hat{\boldsymbol{\rho}}(0)\,\hat{\boldsymbol{U}}^{+}(t)\,, \tag{1.3}$$

with the time evolution unity operator (propagator)

$$\hat{\boldsymbol{U}}(t) = \hat{\boldsymbol{T}}\, e^{\,-i\int_{0}^{t}\hat{\boldsymbol{H}}(t')\,dt'}\,, \tag{1.4}$$

where the Dyson time-ordering operator $\hat{\boldsymbol{T}}$ defines a prescription for evaluating the exponential functions in cases where the Hamiltonians at different times do not commute, $[\hat{\boldsymbol{H}}(t'), \hat{\boldsymbol{H}}(t'')] \neq 0$. For the time independent Hamiltonians $\hat{\boldsymbol{H}}(t) = \hat{\boldsymbol{H}}$ equation (1.4) can be rewritten in the form

$$\hat{\boldsymbol{U}}(t) = e^{-i\hat{\boldsymbol{H}}\,t}\,, \tag{1.5}$$

where time-ordering operator $\hat{\boldsymbol{T}}$ has no more importance. The expectation value of an arbitrary observable operator $\hat{\boldsymbol{A}}$ in the Schrödinger representation can be found

$$\left\langle \hat{\boldsymbol{A}} \right\rangle = \mathbf{Tr}\left\{ \hat{\boldsymbol{A}} \cdot \hat{\boldsymbol{\rho}}(t) \right\} \tag{1.6}$$

by evaluating the trace of the product of the observable operator and density operator.

In most of the cases the complete Hamiltonian $\hat{\boldsymbol{H}}$ of the molecular system is enormously complex, and to derive the exact solutions of equation of motion (1.2) is very complicated. This is a good reason to describe magnetic resonance experiments by a spin Hamiltonian $\hat{\boldsymbol{H}}_S$. It acts only on the spin variables and is obtained by averaging the full Hamiltonian over the lattice coordinates,

$$\hat{\boldsymbol{H}}_S = \mathbf{Tr}_f \left\{ \hat{\boldsymbol{H}} \right\} . \tag{1.7}$$

The nuclear spin Hamiltonian contains only nuclear spin operators and some phenomenological constants [Ern87]. In solid state NMR we are going to distinguish nuclear spin interactions between external fields and internal fields, and the nuclear spin Hamiltonian $\hat{\boldsymbol{H}}_S$ can be written

$$\hat{\boldsymbol{H}}_S = \hat{\boldsymbol{H}}_{ext} + \hat{\boldsymbol{H}}_{int} , \tag{1.8}$$

where

$$\hat{\boldsymbol{H}}_{ext} = \hat{\boldsymbol{H}}_Z + \hat{\boldsymbol{H}}_{RF} \qquad \text{and} \qquad \hat{\boldsymbol{H}}_{int} = \hat{\boldsymbol{H}}_{CS} + \hat{\boldsymbol{H}}_D + \hat{\boldsymbol{H}}_J + \hat{\boldsymbol{H}}_Q , \tag{1.9}$$

where $\hat{\boldsymbol{H}}_Z$, $\hat{\boldsymbol{H}}_{RF}$, $\hat{\boldsymbol{H}}_{CS}$, $\hat{\boldsymbol{H}}_D$, $\hat{\boldsymbol{H}}_J$, and $\hat{\boldsymbol{H}}_Q$ are **Zeeman**, **radio-frequency** field, **chemical shift**, **direct spin-spin**, **indirect spin-spin**, and **quadrupole** interactions, respectively.

If we assume a strong external magnetic field $\vec{\boldsymbol{B}}_0$ ($B_0 \gg 1$ T) thus the **Zeeman** interaction $\hat{\boldsymbol{H}}_Z$ has the dominant contribution to the spin Hamiltonian $\hat{\boldsymbol{H}}_S$:

$$\hat{\boldsymbol{H}}_Z = - \vec{\boldsymbol{M}} \cdot \vec{\boldsymbol{B}}_0 , \tag{1.10}$$

where $\vec{\boldsymbol{M}}$ is the macroscopic magnetization of the nuclear spins I^i. All other terms (except $\hat{\boldsymbol{H}}_Q$) can be written as perturbations. If we assume the orientation of the external magnetic field to the z-direction $\vec{\boldsymbol{B}}_0 = B_0 \, \vec{\boldsymbol{e}}_z$ of a laboratory system, equation (1.10) may be expressed as

$$\hat{\boldsymbol{H}}_Z = - \sum_i \gamma_i B_0 \, \hat{\boldsymbol{I}}_z^i = \sum_i \omega_{0,\,i} \, \hat{\boldsymbol{I}}_z^i , \tag{1.11}$$

where the Larmor frequency $\omega_{0,\,i}$ of spin i is defined through the magnetogyric ratio γ_i and the strength of the external magnetic field

$$\omega_{0,\,i} = - \gamma_i B_0 . \tag{1.12}$$

All measurements in this work were done under the external magnetic field $B_0 = 9.4$ T which corresponds to the Larmor frequency for protons ^1H: $\omega_{0,\,^1H}/2\pi = 400$ MHz and for carbons ^{13}C: $\omega_{0,\,^{13}C}/2\pi = 100$ MHz.

Radio-frequency (r.f.) field interaction $\hat{\boldsymbol{H}}_{RF}$ has the same form as the Zeeman interaction

$$\hat{\boldsymbol{H}}_{RF}(t) = -\sum_i \gamma_i \, \vec{\hat{\boldsymbol{I}}}^{\,i} \cdot \vec{\boldsymbol{B}}_1(t) \,. \tag{1.13}$$

The applied r.f. field $\vec{\boldsymbol{B}}_1$ oscillate with the frequency ω_1 and is normally linearly polarized with the phase φ

$$\vec{\boldsymbol{B}}_1(t) = 2\, B_1 \cos(\omega_1 t) \left[\vec{\boldsymbol{e}}_x \cos\varphi + \vec{\boldsymbol{e}}_y \sin\varphi\right] \,. \tag{1.14}$$

In this conditions equation (1.13) can be written in the form:

$$\hat{\boldsymbol{H}}_{RF}(t) = -\,2\, B_1 \cos(\omega_1 t) \sum_i \gamma_i \Big\{ \hat{\boldsymbol{I}}_x^i \cos\varphi + \hat{\boldsymbol{I}}_y^i \sin\varphi \Big\} \,. \tag{1.15}$$

To solve the density operator equation (1.2), it is advisable to make the r.f. field Hamiltonian time independent by the transformation in to the *rotating frame*. In general a Hamiltonian $\hat{\boldsymbol{H}}(t) = \hat{\boldsymbol{H}}_Z + \hat{\boldsymbol{H}}_1(t)$ can be transformed to the $\hat{\boldsymbol{H}}_Z$-interaction representation by the transformation [SR94]

$$\hat{\boldsymbol{H}}^{\,r} = e^{\,i\hat{\boldsymbol{H}}_Z\, t}\, \hat{\boldsymbol{H}}(t)\, e^{-i\hat{\boldsymbol{H}}_Z\, t} = \hat{\boldsymbol{H}}_Z + e^{\,i\hat{\boldsymbol{H}}_Z\, t}\, \hat{\boldsymbol{H}}_1(t)\, e^{-i\hat{\boldsymbol{H}}_Z\, t} \,. \tag{1.16}$$

The transformation of the r.f. field Hamiltonian to the *rotating frame* as follows from the equation (1.16) can be written as

$$\hat{\boldsymbol{H}}_{RF}^{\,r} = e^{\,i\hat{\boldsymbol{H}}_Z\, t}\, \hat{\boldsymbol{H}}_{RF}(t)\, e^{-i\hat{\boldsymbol{H}}_Z\, t} \,. \tag{1.17}$$

After assumption $\hat{\boldsymbol{H}}_Z = \sum_i \omega_{0,\,i}\, \hat{\boldsymbol{I}}_z^i$ (see equation (1.11)) and the basics trigonometric relations, equation (1.17) may be expressed as

$$\hat{\boldsymbol{H}}_{RF}^{\,r} = -\,2\, B_1 \cos(\omega_1 t) \sum_i \gamma_i \Big\{ \hat{\boldsymbol{I}}_x^i \cos(\omega_{0,\,i}\, t - \varphi) - \hat{\boldsymbol{I}}_y^i \sin(\omega_{0,\,i}\, t - \varphi) \Big\} \,. \tag{1.18}$$

Further mergence of the trigonometric functions in the equation (1.18) will lead to the equation which contains two sets of coefficients $\omega_1 + \omega_{0,\,i}$, $\omega_1 - \omega_{0,\,i}$ as an arguments in the *cos*, *sin* functions, respectively. Choosing $\omega_1 \simeq \omega_{0,\,i}$, the oscillations at frequencies $\omega_1 + \omega_{0,\,i} \simeq 2\,\omega_{0,\,i}$ can be neglected since the nuclear magnetization is influenced appreciably only by fields rotating with the angular frequency close to the nuclear Larmor frequency $\omega_{0,\,i}$. It can be written that

$$\hat{\boldsymbol{H}}_{RF}^{\,r} = -B_1 \sum_i \gamma_i \Big\{ \hat{\boldsymbol{I}}_x^i \cos(\Omega_i\, t + \varphi) + \hat{\boldsymbol{I}}_y^i \sin(\Omega_i\, t + \varphi) \Big\} \,, \tag{1.19}$$

where $\Omega_i = \omega_1 - \omega_{0,\,i}$ is the offset with respect to the carrier frequency ω_1. If the spins are in resonance ($\Omega_i \simeq 0$) the r.f. field Hamiltonian became explicitly time independent and it may be written in the form of

$$\hat{\boldsymbol{H}}^{r}_{RF} = -B_1 \sum_i \gamma_i \Big\{ \hat{\boldsymbol{I}}^{i}_{x} \cos(\varphi) + \hat{\boldsymbol{I}}^{i}_{y} \sin(\varphi) \Big\} \,. \tag{1.20}$$

The **chemical shift** Hamiltonian $\hat{\boldsymbol{H}}_{CS}$ describes the shielding of the nuclear spin from the external $\vec{\boldsymbol{B}}_0$ field by the electron clouds. Due to the strong $\vec{\boldsymbol{B}}_0$ field the orbital angular momentum of the electron cloud is partially aligned in the external field direction which generate local field $\vec{\boldsymbol{B}}_S$ scaled with the $\vec{\boldsymbol{B}}_0$ field, $\vec{\boldsymbol{B}}_S = \tilde{\boldsymbol{\sigma}} \vec{\boldsymbol{B}}_0$. Under such conditions the Hamiltonian of the chemical shift leads ([Meh83], p.11 and Appendix A):

$$\hat{\boldsymbol{H}}_{CS} = \sum_i \gamma_i \, \vec{\hat{\boldsymbol{I}}}^{\,i} \cdot \tilde{\boldsymbol{\sigma}}^{\,i,LF} \cdot \vec{\boldsymbol{B}}_0 = - \sum_i \omega_{0,\,i} \, \Big\{ \hat{\boldsymbol{I}}^{i}_{x} \, \sigma^{i,LF}_{xz} + \hat{\boldsymbol{I}}^{i}_{y} \, \sigma^{i,LF}_{yz} + \hat{\boldsymbol{I}}^{i}_{z} \, \sigma^{i,LF}_{zz} \Big\} \,. \tag{1.21}$$

The $\vec{\boldsymbol{B}}_0$ field was chosen to the z-direction (0,0,B_0). The $\tilde{\boldsymbol{\sigma}}^{\,i,LF}$ represent the chemical-shift (CS) tensor in the laboratory-frame representation with elements $\tilde{\boldsymbol{\sigma}}^{\,i,LF}_{\alpha\beta}$ $(\alpha, \beta = x, y, z)$. In the case of high external fields ($B_0 \gg 1$ T), local fields felt by ^{1}H, ^{2}H, ^{13}C, ^{15}H, ^{19}F, ^{29}Si, or ^{31}P nuclei are smaller compared with B_0 field and CS Hamiltonian (equation (1.21)) can be simplified assuming first-order perturbation theory so

$$\hat{\boldsymbol{H}}_{CS} = - \sum_i \omega_{0,\,i} \hat{\boldsymbol{I}}^{i}_{z} \, \sigma^{i,LF}_{zz} \,. \tag{1.22}$$

The asymmetric components $\frac{1}{2}\,(\tilde{\boldsymbol{\sigma}} - \tilde{\boldsymbol{\sigma}}^{\mathrm{T}})$ of the CS tensor $\tilde{\boldsymbol{\sigma}}$ contribute to the resonance frequency shift only in the second order and can be usually neglected ([Meh83], Appendix C). The symmetric part of the CS tensor $\frac{1}{2}\,(\tilde{\boldsymbol{\sigma}} + \tilde{\boldsymbol{\sigma}}^{\mathrm{T}})$ is characterized most conveniently in the coordinate system in which it is diagonal. This is the 'principal axes system' (PAS). For polar coordinate system where φ and ϑ are the polar coordinates of $\vec{\boldsymbol{B}}_0$ in PAS, equation (1.22) with the CS tensor $\tilde{\boldsymbol{\sigma}}$ and its eigenvalues $\sigma^{\mathrm{PAS}}_{xx}$, $\sigma^{\mathrm{PAS}}_{yy}$, and $\sigma^{\mathrm{PAS}}_{zz}$, may be for a single spin written [SR94] as

$$\hat{\boldsymbol{H}}_{CS} = \big\{ -\omega_0 \, \sigma_{iso} + \tfrac{1}{2}\,\delta\,(3\,\cos^2\vartheta - 1 - \eta \sin^2\vartheta\,\cos 2\varphi) \big\}\, \hat{\boldsymbol{I}}_z \,, \tag{1.23}$$

where

$$\begin{aligned} \sigma_{iso} &= \tfrac{1}{3}\,\big\{ \sigma^{\mathrm{PAS}}_{xx} + \sigma^{\mathrm{PAS}}_{yy} + \sigma^{\mathrm{PAS}}_{zz} \big\} \\ \delta &= -\,\omega_0\,\big(\sigma^{\mathrm{PAS}}_{zz} - \sigma_{iso} \big) \\ \eta &= \frac{\sigma^{\mathrm{PAS}}_{yy} - \sigma^{\mathrm{PAS}}_{xx}}{\sigma^{\mathrm{PAS}}_{zz} - \sigma_{iso}} \end{aligned} \tag{1.24}$$

are the isotropic chemical shift parameter, the anisotropy parameter and the asymmetry parameter, respectively. The first part of the equation (1.23) corresponds to an isotropic frequency and the second part to an anisotropic frequency. To make the CS interaction independent on the magnetic field B_0 it is useful to measure it in dimensionless units independent to each nucleus ($\omega_{0,\,i}\,.\,10^{-6}$). The scale is called ppm-scale. The typical values for protons ^{1}H lays between 0 and 10 ppm.

The **direct spin-spin** interaction among spin i and j can be described by **dipolar** Hamiltonian $\hat{\boldsymbol{H}}_D$ according to the Correspondence Principle

$$\hat{\boldsymbol{H}}_D = -\sum_{i<j} \frac{\mu_0\hbar}{4\pi}\,\gamma_i\gamma_j \frac{3\left(\vec{\hat{\boldsymbol{I}}}^{\,i}\cdot\vec{\boldsymbol{e}}_r^{\,ij}\right)\left(\vec{\hat{\boldsymbol{I}}}^{\,j}\cdot\vec{\boldsymbol{e}}_r^{\,ij}\right) - \vec{\hat{\boldsymbol{I}}}^{\,i}\cdot\vec{\hat{\boldsymbol{I}}}^{\,j}}{\left|\vec{\boldsymbol{r}}_{ij}\right|^3} \tag{1.25}$$

$$= \sum_{i<j} \vec{\hat{\boldsymbol{I}}}^{\,i}\cdot\tilde{\boldsymbol{D}}^{\,ij}\cdot\vec{\hat{\boldsymbol{I}}}^{\,j}\,, \tag{1.26}$$

where $\vec{\boldsymbol{r}}_{ij}$ determines the vector from nucleus i to nucleus j with its basis vector $\vec{\boldsymbol{e}}_r^{\,ij} = \vec{\boldsymbol{r}}_{ij}/\left|\vec{\boldsymbol{r}}_{ij}\right|$. $\tilde{\boldsymbol{D}}^{\,ij}$ represents the dipolar coupling tensor in the appropriate base defined through $\vec{\boldsymbol{e}}_r^{\,ij}$ vector. The dipolar-coupling constant is measured in the angular frequency units and is defined as

$$d_{ij} = \frac{\mu_0\hbar}{4\pi}\,\frac{\gamma_i\gamma_j}{r_{ij}^3}\,. \tag{1.27}$$

For example, we calculate that for $^1\mathrm{H}-{}^1\mathrm{H}$ spin pair in a CH_2 group ($\gamma_{^1\mathrm{H}} = 2.675\times10^8\ \mathrm{T^{-1}s^{-1}}$) with a distance of 1.8 Å (0.18 nm), the coupling strength is $d_{^1\mathrm{H}-{}^1\mathrm{H}} = 105.4\ \mathrm{kHz}\times(2.675)^2/(1.8)^3 = 2\,\pi\times 20.6\ \mathrm{kHz}$. In the case of high static field (similar like for the CS interaction) only those components of the Hamiltonian contribute to the spectrum in the first order approximation which are time independent and the Hamiltonian defined by equation (1.25) can be truncated. For homonuclear dipolar interactions between spins I^i the truncated Hamiltonian can be written [Meh83] as

$$\hat{\boldsymbol{H}}_D^{\,II} = -\sum_{i<j} d_{ij}^{II}\,\tfrac{1}{2}\left(3\cos^2\vartheta_{ij}-1\right)\left(3\,\hat{\boldsymbol{I}}_z^{\,i}\hat{\boldsymbol{I}}_z^{\,j} - \vec{\hat{\boldsymbol{I}}}^{\,i}\cdot\vec{\hat{\boldsymbol{I}}}^{\,j}\right). \tag{1.28}$$

Angle ϑ_{ij} is the angle between the magnetic field B_0 and the vector $\vec{\boldsymbol{e}}_r^{\,ij}$ connecting spin I^i and I^j (Index $\{II\}$ on the dipolar-coupling constant d_{ij} represent the equivalence of nuclei: $\gamma_i = \gamma_j = \gamma_I$). The truncated Hamiltonian of heteronuclear dipolar couplings is given by (I^i and S^i spins)

$$\hat{\boldsymbol{H}}_D^{\,IS} = -\sum_{i,j} d_{ij}^{IS}\,\tfrac{1}{2}\left(3\cos^2\vartheta_{ij}-1\right)2\,\hat{\boldsymbol{I}}_z^{\,i}\hat{\boldsymbol{S}}_z^{\,j}\,. \tag{1.29}$$

The **indirect spin-spin** coupling (J-coupling), which result from electron-nuclear interactions have the form

$$\hat{\boldsymbol{H}}_J = -\sum_{i<j} \vec{\hat{\boldsymbol{I}}}^{\,i} \cdot \tilde{\boldsymbol{J}}^{\,ij} \cdot \vec{\hat{\boldsymbol{I}}}^{\,j}\,, \tag{1.30}$$

where $\tilde{\boldsymbol{J}}^{\,ij}$ is the indirect spin-spin coupling tensor. On contrary to the direct coupling between spins (dipolar coupling) the J-coupling provide an information about the connectivities of the electron clouds surrounding nuclei to the neighboured nuclear spins I^i. Usually it is very weak ($\approx$ 100Hz) and in the solid-state NMR it can be neglected. In liquids, in the case of high static external field B_0 only the scalar component of the J-coupling tensor ($J_{ij} = \frac{1}{3}\mathrm{Tr}\{\tilde{\boldsymbol{J}}\}$) contribute to the spectrum and the time independent part of the Hamiltonian 'secular part' reads:

$$\hat{\boldsymbol{H}}_J = -\sum_{i<j} J_{ij}\, \hat{\boldsymbol{I}}^i_z\, \hat{\boldsymbol{I}}^j_z\,. \tag{1.31}$$

Nuclei with $I^i \geq 1$ generates electric field gradients with the nuclear **quadrupole** moment Q^i and their interaction with other nuclei can be described by the Hamiltonian

$$\hat{\boldsymbol{H}}_Q = \sum_i \frac{eQ^i}{2I^i(2I^i-1)\hbar}\, \vec{\hat{\boldsymbol{I}}}^{\,i} \cdot \tilde{\boldsymbol{V}}^{\,i} \cdot \vec{\hat{\boldsymbol{I}}}^{\,i}\,, \tag{1.32}$$

where $\tilde{\boldsymbol{V}}^{\,i}$ is the electric field gradient tensor at the site of nucleus i and e is the elementary charge. After averaging ($B_0 \gg 1$ T) the secular part of the **quadrupolar** Hamiltonian can be written in the form [SR94] of

$$\hat{\boldsymbol{H}}_Q = \sum_i \frac{eQ^i}{2I^i(2I^i-1)\hbar}\, V^{i,\,LF}_{zz}\, \tfrac{1}{2}\left(3\,\hat{\boldsymbol{I}}^{\,i}_z\, \hat{\boldsymbol{I}}^{\,i}_z - \vec{\hat{\boldsymbol{I}}}^{\,i} \cdot \vec{\hat{\boldsymbol{I}}}^{\,i}\right). \tag{1.33}$$

Typical values for quadrupolar coupling are in the range 200 kHz−2 GHz (Br, I, As, ...). In this work the quadrupolar coupling has no importance because we were concentrated to the nuclei with spin $I = \frac{1}{2}$ and in such cases it vanishes.

1.2 Equilibrium density operator

The density operator represents a valid synthesis of quantum mechanics with statistical mechanics. In thermal equilibrium at a temperature T and with Hamiltonian $\hat{\boldsymbol{H}}$ of the system, the density operator of the spin system is analogous to the classical Boltzmann distribution (we will reintroduce for a moment $\hbar$ into Hamiltonian $\hat{\boldsymbol{H}}$ in order to obtain unitless ratio $\hbar\gamma B_0/k_BT$)

$$\hat{\boldsymbol{\rho}}_{eq} = \frac{e^{-\hbar\hat{\boldsymbol{H}}/k_BT}}{Z} \qquad \text{with} \qquad Z = \mathbf{Tr}\left\{e^{-\hbar\hat{\boldsymbol{H}}/k_BT}\right\}, \tag{1.34}$$

where k_B is the Boltzmann constant. The dominant contribution to the spin Hamiltonian $\hat{\boldsymbol{H}}$ has the Zeeman interaction (equation (1.11)) for a B_0 fields stronger than 1 Tesla and for individual spins can be written

$$\hat{\boldsymbol{\rho}}_{eq}^{i} = \frac{e^{-\frac{\hbar\,\omega_{0,\,i}}{k_B T}\hat{\boldsymbol{I}}_z^{\,i}}}{Z^i}\,. \tag{1.35}$$

At temperatures above 1 K in the fields currently available $|\hbar\,\omega_0| \gg k_B T$, exponential function in equation (1.35) can be expanded so that the quadratic and all higher terms vanish compared to the linear term

$$e^{-\frac{\hbar\,\omega_{0,\,i}}{k_B T}\hat{\boldsymbol{I}}_z^{\,i}} \simeq \hat{\mathbb{1}}^{\,i} - \frac{\hbar\,\omega_{0,\,i}}{k_B T}\hat{\boldsymbol{I}}_z^{\,i}\,. \tag{1.36}$$

The denominator of equation (1.35) corresponds to all possible states of the system $2I^i+1$ and for N equivalent spins equilibrium density operator takes a form

$$\hat{\boldsymbol{\rho}}_{eq} \simeq \frac{N}{(2I+1)^N}\left(\hat{\mathbb{1}} - \frac{\hbar\,\omega_0}{k_B T}\hat{\boldsymbol{I}}_z\right)\,. \tag{1.37}$$

The unity operator $\hat{\mathbb{1}}$ commutes with all operators and is irrelevant in most cases. According to equation (1.37) it can be defined the initial density operator of the system so

$$\hat{\boldsymbol{\rho}}(0) \stackrel{\text{def}}{=} c\hat{\boldsymbol{I}}_z\,, \tag{1.38}$$

where $c = -\hbar\,\omega_0/k_B T$.

1.3 Average Hamiltonian theory

In NMR the spin interaction Hamiltonian is usually time-dependent and it is much more convenient to describe an experiment by the average Hamiltonian ([Hae76]) which represent the 'average' motion of the spin system. Most of the multiple quantum experiments can be described by an average Hamiltonian theory and this is the goal of this work.

In general the Hamiltonian in the rotating frame is split into two parts (equation (1.8))

$$\hat{\boldsymbol{H}} = \hat{\boldsymbol{H}}_{ext}(t) + \hat{\boldsymbol{H}}_{int}\,, \tag{1.39}$$

where $\hat{\boldsymbol{H}}_{ext}$ and $\hat{\boldsymbol{H}}_{int}$ are defined by the equation (1.9). To find the solution for the density operator equation (equation (1.2)) one has to derive the time evolution propagator

$$\hat{\boldsymbol{U}}(t) = \hat{\boldsymbol{T}}\, e^{\,-i\int\limits_0^t dt'\left(\hat{\boldsymbol{H}}_{ext}(t')+\hat{\boldsymbol{H}}_{int}\right)}\,. \tag{1.40}$$

$\hat{\boldsymbol{T}}$ is the Dyson time-ordering operator (see also equation (1.4)) defined through the following relations

$$\hat{\boldsymbol{T}}\left\{\hat{\boldsymbol{H}}(t_1)\hat{\boldsymbol{H}}(t_2)\right\} = \begin{cases} \hat{\boldsymbol{H}}(t_1)\hat{\boldsymbol{H}}(t_2) & \text{for} \quad t_1 > t_2 \\ \hat{\boldsymbol{H}}(t_2)\hat{\boldsymbol{H}}(t_1) & \text{for} \quad t_1 < t_2\,. \end{cases} \tag{1.41}$$

Now we attempt to separate the effects of explicitly time-independent Hamiltonian $\hat{\boldsymbol{H}}_{int}$ and time-dependent Hamiltonian $\hat{\boldsymbol{H}}_{ext}(t)$ and to divide the propagator from the equation (1.40) into two products

$$\hat{\boldsymbol{U}}(t) = \hat{\boldsymbol{U}}_1(t)\hat{\boldsymbol{U}}_{int}(t) \tag{1.42}$$

with

$$\hat{\boldsymbol{U}}_1(t) = \hat{\boldsymbol{T}}\, e^{-i\int_0^t \hat{\boldsymbol{H}}_{ext}(t')\,dt'} \tag{1.43}$$

and

$$\hat{\boldsymbol{U}}_{int}(t) = \hat{\boldsymbol{T}}\, e^{-i\int_0^t \hat{\tilde{\boldsymbol{H}}}(t')\,dt'}\,, \tag{1.44}$$

where $\hat{\boldsymbol{U}}_1(t)$ depends only on the perturbation $\hat{\boldsymbol{H}}_{ext}(t)$. $\hat{\tilde{\boldsymbol{H}}}(t)$ in equation (1.44) is the Hamiltonian in the time-dependent interaction representation with respect to $\hat{\boldsymbol{H}}_{ext}(t)$, often called the *toggling frame*. To assume $\hat{\boldsymbol{H}}$ Hermitan it follows $\hat{\boldsymbol{U}}^{+}(t) = \hat{\boldsymbol{U}}^{-1}(t)$ and the initially time-dependent toggling frame Hamiltonian can be written

$$\hat{\tilde{\boldsymbol{H}}}(t) = \hat{\boldsymbol{U}}_1^{-1}(t)\,\hat{\boldsymbol{H}}_{int}\,\hat{\boldsymbol{U}}_1(t)\,. \tag{1.45}$$

We can further assume, that the external field may be periodic with a period τ_c i.e.

$$\hat{\boldsymbol{H}}_{ext}(t + n\,\tau_c) = \hat{\boldsymbol{H}}_{ext}(t); \quad n = 0, 1, 2, \ldots \tag{1.46}$$

which is for our cases good fulfilled (see chapter 2). From equation (1.46) follows

$$\hat{\boldsymbol{U}}_1(n\,\tau_c) = \hat{\boldsymbol{U}}_1^{n}(\tau_c) \tag{1.47}$$

and it also leads to a periodicity of toggling frame Hamiltonian with

$$\hat{\tilde{\boldsymbol{H}}}(t) = \hat{\tilde{\boldsymbol{H}}}(t + n\,\tau_c) \tag{1.48}$$

and

$$\hat{\boldsymbol{U}}_{int}(n\,\tau_c) = \hat{\boldsymbol{U}}_{int}^{n}(\tau_c)\,. \tag{1.49}$$

If in addition the external field is cyclic in the sense

$$\hat{\boldsymbol{U}}_1(\tau_c) = \hat{\mathbb{1}}\,, \tag{1.50}$$

the general propagator $\hat{\boldsymbol{U}}(\tau_c)$ (equation (1.42)) is described by the one cycle propagator $\hat{\boldsymbol{U}}_{int}(\tau_c)$ i.e.

$$\hat{\boldsymbol{U}}(\tau_c) = \hat{\boldsymbol{U}}_{int}(\tau_c) \qquad \text{and} \qquad \hat{\boldsymbol{U}}(n\,\tau_c) = \hat{\boldsymbol{U}}^n_{int}(\tau_c)\,. \tag{1.51}$$

Our goal is to express equation (1.44) in the sense

$$\hat{\boldsymbol{U}}_{int}(\tau_c) = e^{-i\hat{\bar{\boldsymbol{H}}}\tau_c}\,, \tag{1.52}$$

where $\hat{\bar{\boldsymbol{H}}}$ is an average Hamiltonian and it can be divided into contributions from different orders

$$\hat{\bar{\boldsymbol{H}}} = \hat{\bar{\boldsymbol{H}}}^{(0)} + \hat{\bar{\boldsymbol{H}}}^{(1)} + \hat{\bar{\boldsymbol{H}}}^{(2)} + \dots\,. \tag{1.53}$$

Using Magnus expansion [Ern87] which forms the basis of average Hamiltonian theory it can be written

$$\hat{\bar{\boldsymbol{H}}}^{(0)} = \frac{1}{\tau_c}\int_0^{\tau_c} dt\,\hat{\tilde{\boldsymbol{H}}}(t) \tag{1.54}$$

$$\hat{\bar{\boldsymbol{H}}}^{(1)} = \frac{-i}{2\tau_c}\int_0^{\tau_c} dt_2 \int_0^{t_2} dt_1 [\hat{\tilde{\boldsymbol{H}}}(t_2), \hat{\tilde{\boldsymbol{H}}}(t_1)] \tag{1.55}$$

$$\hat{\bar{\boldsymbol{H}}}^{(2)} = -\frac{1}{6\tau_c}\int_0^{\tau_c} dt_3 \int_0^{t_3} dt_2 \int_0^{t_2} dt_1 \Big\{[\hat{\tilde{\boldsymbol{H}}}(t_3), [\hat{\tilde{\boldsymbol{H}}}(t_2), \hat{\tilde{\boldsymbol{H}}}(t_1)]] + [\hat{\tilde{\boldsymbol{H}}}(t_1), [\hat{\tilde{\boldsymbol{H}}}(t_2), \hat{\tilde{\boldsymbol{H}}}(t_3)]]\Big\}\,. \tag{1.56}$$

In most cases multiple-pulse sequences are designed to remove higher terms $\hat{\bar{\boldsymbol{H}}}^{(1)}, \dots$ from average Hamiltonian and only zero-order $\hat{\bar{\boldsymbol{H}}}^{(0)}$ term survive. Zero-order term has a particularly simple form. It is just the time average of the toggling frame Hamiltonian $\hat{\tilde{\boldsymbol{H}}}(t)$ and it has the most importance for the multiple-pulse sequences which we will investigate in this work.

1.4 Dipolar interaction and irreducible tensors

In this section we would like to represent dipolar Hamiltonian introduced at the page 10 in another form i.e. with the help of irreducible spherical tensors. This representation of spin Hamiltonian is much more convenient in the case of magic-angle-spinning experiment described in the section 1.6.

The spin interaction Hamiltonian may be expressed in the terms of irreducible spherical tensors as [Meh83, Spi78, SR94]

$$\hat{\boldsymbol{H}} = \sum_{k=0}^{2} \sum_{q=-k}^{+k} (-1)^q \, A_{k,q} \hat{\boldsymbol{T}}_{k,-q} \,, \tag{1.57}$$

where $A_{k,q}$ contains all lattice and $\hat{\boldsymbol{T}}_{k,q}$ all spin variables. Due to the fact that the spin interactions in NMR are expressed by second rank tensors the summation in equation (1.57) goes only until $k = 2$. In the high field case ($B_0 \gg 1$ T) all terms with $q \neq 0$ are neglected in the first order approximation and only secular terms ($q = 0$) remains. In addition antisymmetric part with $k = 1$ of spin interactions does not contribute to the spectrum in the first order and can also be neglected ([Meh83] p.41). Under these conditions equation (1.57) is reduced to

$$\hat{\boldsymbol{H}}^{(0)} = A_{0,0} \hat{\boldsymbol{T}}_{0,0} + A_{2,0} \hat{\boldsymbol{T}}_{2,0} \,. \tag{1.58}$$

In the case of dipolar coupling due to the symmetry of dipolar coupling tensor $\tilde{\boldsymbol{D}}$ $A_{0,0} = 0$ ($A_{0,0} = -\frac{1}{\sqrt{3}} \mathbf{Tr}\{D_{ij}\}$) and equation (1.58) for homonuclear coupling may be expressed in the form[1]

$$\hat{\boldsymbol{H}}_D = -\sum_{i<j} d_{ij}^{II} \, R_{2,0}^{ij} \hat{\boldsymbol{T}}_{2,0}^{ij} \tag{1.59}$$

with

$$R_{2,0}^{ij} = \sqrt{\tfrac{3}{2}} \left(3\cos^2 \vartheta_{ij} - 1\right) \tag{1.60}$$

$$\hat{\boldsymbol{T}}_{2,0}^{ij} = \tfrac{1}{\sqrt{6}} \left(3 \, \hat{\boldsymbol{I}}_z^{\,i} \hat{\boldsymbol{I}}_z^{\,j} - \vec{\hat{\boldsymbol{I}}}^{\,i} \cdot \vec{\hat{\boldsymbol{I}}}^{\,j}\right) . \tag{1.61}$$

$R_{2,0}^{ij}$ contains only pure geometrical variables and d_{ij}^{II} is the dipolar-coupling constant defined by equation (1.27). With the help of spherical harmonics $Y_{2,q}$, geometrical parameter $R_{2,q}$ can be defined in more general way

$$R_{2,q} = \sqrt{\tfrac{24\,\pi}{5}} \; Y_{2,q} \,. \tag{1.62}$$

Definitions of $Y_{k,q}$ can be found in [SR94] p.451.

[1] We will not use the mark (0) for secular dipolar Hamiltonian to prevent interchange it with zero order average Hamiltonian using in Magnus expansion series (see equation (1.54))

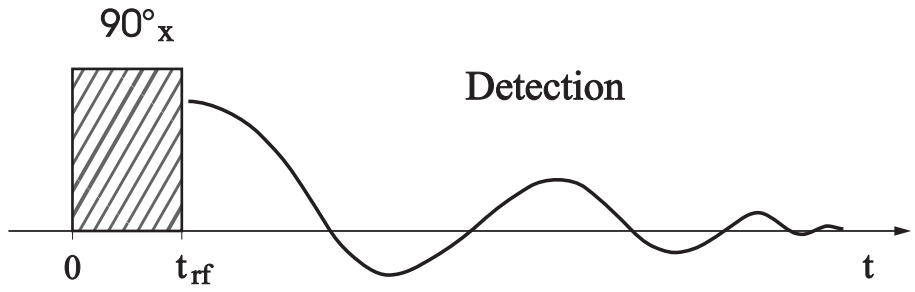

Figure 1.1: *Schematic picture of one pulse experiment. The r.f. pulse is oriented in x-direction and rotates the magnetization in rotating frame about 90^o ($\frac{\pi}{2}$).*

1.5 One pulse experiment

The most simplest experiment in NMR is an one pulse experiment, schematically showed in Figure 1.1. The interactions between spins can be detected in the detection period just after the excitation of the system with the r.f. pulse in detection period. To describe an experiment we will assume an ensemble of equivalent spins $I^i = \frac{1}{2}$ where the initial state of the system is defined through the initial density operator (equation (1.38)). The effect of r.f. pulse in the rotating frame is described by the equation (1.20) and using equations (1.3−1.5) the density operator just after the r.f. pulse applied in the x-direction has the form

$$\hat{\boldsymbol{\rho}}(t_{\rm rf}) = e^{\,i\gamma B_1 t_{\rm rf}\hat{\boldsymbol{I}}_x}\, c\hat{\boldsymbol{I}}_z\, e^{-i\gamma B_1 t_{\rm rf}\hat{\boldsymbol{I}}_x}\,. \tag{1.63}$$

If the strength B_1 and the duration $t_{\rm rf}$ of the r.f. pulse matches the condition

$$\gamma B_1 t_{\rm rf} = \frac{\pi}{2}, \tag{1.64}$$

the pulse rotate the magnetization about 90^0 (left handed sense rotation around x-axis using the definitions in equation (1.20) and (1.11)) equation (1.63) may be rewritten

$$\hat{\boldsymbol{\rho}}(t_{\rm rf}) = \hat{\boldsymbol{\rho}}(0^+) = c\hat{\boldsymbol{I}}_y\,. \tag{1.65}$$

The state prepared by the initial pulse now decays due to the Zeeman interaction an internal spin interaction according to the Liouville-von Neumann equation

$$\frac{d}{dt}\,\hat{\boldsymbol{\rho}}(t) = -i[\hat{\boldsymbol{H}}_Z + \hat{\boldsymbol{H}}_{int}, \hat{\boldsymbol{\rho}}(t)] \tag{1.66}$$

and the NMR decay signal can be obtained in the α ($\alpha = x, y$) direction of the rotating frame as

$$S_\alpha(t) = \frac{\mathbf{Tr}\left\{\,\hat{\boldsymbol{I}}_\alpha\hat{\boldsymbol{\rho}}(t)\right\}}{\mathbf{Tr}\left\{\hat{\boldsymbol{I}}_z\hat{\boldsymbol{\rho}}(0)\right\}}\,. \tag{1.67}$$

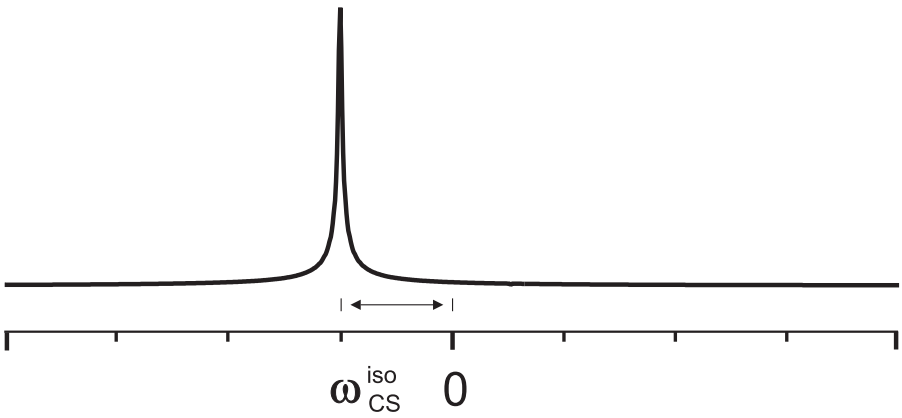

Figure 1.2: *The shift of frequency due to isotropic chemical shift interaction.*

Let us assume only isotropic chemical shift interaction ($\omega_{CS}^{iso} = \omega_0 \sigma_{iso}$) from internal Hamiltonian $\hat{\boldsymbol{H}}_{int}$. The density operator for a single spin after the x-pulse at $t > t_{\mathrm{rf}}$ can be found

$$\begin{aligned} \hat{\boldsymbol{\rho}}(t) &= e^{i\omega_{CS}^{iso} t\, \hat{\boldsymbol{I}}_z}\, \hat{\boldsymbol{\rho}}(0^+) e^{-i\omega_{CS}^{iso} t\, \hat{\boldsymbol{I}}_z} \\ &= c\left[\hat{\boldsymbol{I}}_y \cos(\omega_{CS}^{iso} t) + \hat{\boldsymbol{I}}_x \sin(\omega_{CS}^{iso} t)\right] . \end{aligned} \tag{1.68}$$

To evaluate the NMR signal from equation (1.68), which corresponds to the magnetization, with the help of equation (1.67) we will get

$$S_y(t) = \cos(\omega_{CS}^{iso} t) \tag{1.69}$$

and

$$S_x(t) = \sin(\omega_{CS}^{iso} t) \tag{1.70}$$

for a signal detected in the y,x-direction, respectively. Due to the strong magnetic field B_0 applied to the system, NMR signal relax with the typical relaxation time T_2 and is called FID (*free induction decay*). In modern NMR spectrometers the acquisition of both signals (equation (1.69) and (1.70)) at the same time often called *quadrature detection* is possible. After digitalization and complex fourier transformation of the data we will get a spectrum shown in Figure 1.2.

1.6 Magic Angle Spinning

One of the experimental technique to improve the resolution of NMR spectra is *magic-angle-spinning* (MAS). The sample rotates about an axis which is tilted by an angle ϑ_m

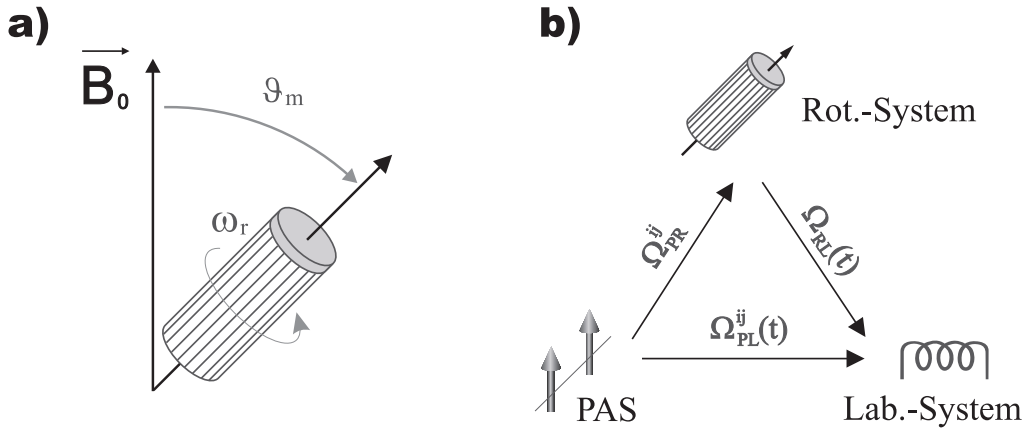

Figure 1.3: a) *Schematic description of MAS where rotor axis is tilted from the* $\vec{\boldsymbol{B}}_0$ *field by the angle* $\vartheta_m = 54.7°$. b) *Relative orientation of PAS and LabS under sample rotation described by the angle* $\Omega^{ij}_{PL}(t)$*, which is built up by two successive rotational transformations with angles* Ω^{ij}_{PR} *and* $\Omega_{RL}(t)$.

(called '*magic angle*') with respect to the magnetic field $\vec{\boldsymbol{B}}_0$ (see Figure 1.3a). It was noted independently by Andrew ([And58]) and Lowe ([Low58]) that in such a case dipolar interactions and chemical shift anisotropy are averaged out from the spectrum and usually only narrow isotropic lines remains. If the spinning rate ω_r of the sample is much larger than the anisotropic spin interaction the spinning sidebands[2] are well separated from the isotropic lines and became vanishingly small with increasing ω_r. We are going to consider only dipolar spin interactions in this section because this is of main interest in this work.

To derive dipolar Hamiltonian under MAS lets start with a little bit different representation of geometrical part of the Hamiltonian used in equations (1.59) and (1.60)

$$R^{ij}_{2,0} = \sqrt{6}\ \mathcal{D}^{(2)}_{0,0}(\Omega^{ij}_{PL})\,, \tag{1.71}$$

where the Wigner rotation matrices $\mathcal{D}^{(2)}_{k,q}$ can be found in Appendix B. The Euler angle $\Omega^{ij}_{PL} = (\varphi^{ij}_{PL}, \vartheta^{ij}_{PL}, \psi^{ij}_{PL})$ specify the relative orientation of two coordinate systems i.e. *Principle axis system* (PAS) and *Laboratory system* (LabS). If the sample rotate about an axis tilted by an angle ϑ_{RL} from the main field $\vec{\boldsymbol{B}}_0$ director the geometrical part $R^{ij}_{2,0}$ became time dependent $R^{ij}_{2,0}(t)$. It is convenient to describe it by two successive rotations (see Figure 1.3b) and by the time dependent rotation matrix $\mathcal{D}^{(2)}_{0,0}(t)$. According to

[2]Additional lines in the spectrum originating from the sample rotation, separated from the isotropic line exactly at the rotor frequency intervals.

equation (B.2) it can be written as

$$\mathcal{D}^{(2)}_{0,0}(\Omega^{ij}_{PL}(t)) = \sum_{q=-2}^{2} \mathcal{D}^{(2)}_{0,q}(\Omega^{ij}_{PR})\, \mathcal{D}^{(2)}_{q,0}(\Omega_{RL}(t))\,, \tag{1.72}$$

where Ω^{ij}_{PR} corresponds to the relative orientation of PAS and *Rotor system* and $\Omega_{RL}(t)$ describe the rotation of the rotor seen from the *Laboratory system* through the Wigner matrices (see equation (B.1))

$$\mathcal{D}^{(2)}_{q,0}(\Omega_{RL}(t)) = e^{-iq\,\varphi_{RL}(t)}\, d^{(2)}_{q,0}(\vartheta_{RL})\,. \tag{1.73}$$

Factors $d^{(2)}_{q,0}$ are defined in Table B.1. Due to the fix angle ϑ_{RL} in *Rotor system* the time dependence in equation (1.73) is introduced through an angle $\varphi_{RL}(t) = \varphi_0 + \omega_r\, t$ with the starting point φ_0. Combining equations (1.71−1.73) we will get

$$R^{ij}_{2,0}(t) = \sum_{q=-2}^{2} \sqrt{6}\ \mathcal{D}^{(2)}_{0,q}(\Omega^{ij}_{PR})\, e^{-iq\,\varphi_0}\, d^{(2)}_{q,0}(\vartheta_{RL})\, e^{-iq\,\omega_r\, t}\,, \tag{1.74}$$

where $R^{ij}_{2,0}(t)$ describes the time dependence of dipolar Hamiltonian:

$$\hat{\boldsymbol{H}}_D(t) = -\sum_{i<j} d^{II}_{ij}\, R^{ij}_{2,0}(t)\, \hat{\boldsymbol{T}}^{ij}_{2,0}\,. \tag{1.75}$$

It is immediately evident from equation (1.74) that rotational sidebands appear at multiples of the frequency ω_r and $2\omega_r$ away from the central isotropic lines (see Figure 1.4). Before proofing this aspect further, let us go back to the rapid spinning case. If ω_r is very large ($\omega_r \gg ||\hat{\boldsymbol{H}}_D||$) or stroboscopic observation at time intervals $\tau = n\, 2\pi/\omega_r$ is performed, only the time independent part (with $q = 0$) of $R^{ij}_{2,0}(t)$ in equation (1.74) survives, i.e.

$$\bar{R}^{ij}_{2,0} = d^{(2)}_{0,0}(\vartheta_{RL})\, R_{2,0}(\Omega^{ij}_{PR})\,. \tag{1.76}$$

In this case, the time independent dipolar Hamiltonian

$$\hat{\bar{\boldsymbol{H}}}_D = -\tfrac{1}{2}\left(3\,\cos^2\vartheta_{RL} - 1\right) \sum_{i<j} d^{II}_{ij}\, R_{2,0}(\Omega^{ij}_{PR})\, \hat{\boldsymbol{T}}^{ij}_{2,0} \tag{1.77}$$

governs the spectrum. It is evident from equation (1.77) that for the angle $\vartheta_{RL} := \vartheta_m = \arccos(\sqrt{\tfrac{1}{3}}) \doteq 54.7°$ called '*magic angle*' the dipolar coupling Hamiltonian vanish and only isotropic part of the secular Hamiltonian remain ([Meh83]).

In the case of moderate spinning speed $\omega_r \simeq ||\hat{\boldsymbol{H}}_D||$ dipolar coupling influence the spectrum and the spinning sidebands become visible. Analytical description of this situation is for the behaviour of the spin system with many spins usually very complicated due

to the complexity of the dipolar Hamiltonian in equation (1.75). Therefore it will be made only for two dipolar coupled spins-½. After applying 90°-pulse in the x-direction of the rotating frame the initial state of the system for I^i and I^j spins is according to equation (1.65) given by

$$\hat{\boldsymbol{\rho}}(0^+) = c\left(\hat{\boldsymbol{I}}_y^i + \hat{\boldsymbol{I}}_y^j\right). \tag{1.78}$$

The time evolution of the density matrix is described by the Liouville-von Neumann equation (1.2) with its formal solution in equation (1.3). The Dyson time-ordering operator in equation (1.4) has for two spin system no importance and the Liouville-von Neumann equation can be formally solved (see also Table A.1 and equation (A.4)):

$$\begin{aligned}
\hat{\boldsymbol{\rho}}(t) &= e^{-i\int_0^t \hat{\boldsymbol{H}}_D(t')\,dt'}\,\hat{\boldsymbol{\rho}}(0^+)\,e^{i\int_0^t \hat{\boldsymbol{H}}_D(t')\,dt'} \\
&= c\,e^{i\int_0^t dt'\,d_{ij}^{II}R_{2,0}^{ij}(t')\hat{\boldsymbol{T}}_{2,0}^{ij}}\left(\hat{\boldsymbol{I}}_y^i + \hat{\boldsymbol{I}}_y^j\right)e^{-i\int_0^t dt'\,d_{ij}^{II}R_{2,0}^{ij}(t')\hat{\boldsymbol{T}}_{2,0}^{ij}} \\
&= c\left(\hat{\boldsymbol{I}}_y^i + \hat{\boldsymbol{I}}_y^j\right)\cos\left[\int_0^t \omega_D^{ij}(t')\,dt'\right] - 2c\left(\hat{\boldsymbol{T}}_{2,1}^{ij} - \hat{\boldsymbol{T}}_{2,-1}^{ij}\right)\sin\left[\int_0^t \omega_D^{ij}(t')\,dt'\right]
\end{aligned} \tag{1.79}$$

with

$$\omega_D^{ij}(t) = \sqrt{\tfrac{3}{8}}\,d_{ij}^{II}R_{2,0}^{ij}(t)\,. \tag{1.80}$$

The products with $\hat{\boldsymbol{T}}_{2,\pm1}^{ij}$ have no influence on the signal detected in $\alpha = x, y$ direction of the rotating frame because their trace vanish

$$\mathbf{Tr}\left\{\hat{\boldsymbol{I}}_\alpha^i\,\hat{\boldsymbol{T}}_{2,\pm1}^{ij}\right\} = \mathbf{Tr}\left\{\hat{\boldsymbol{I}}_\alpha^j\,\hat{\boldsymbol{T}}_{2,\pm1}^{ij}\right\} = 0 \tag{1.81}$$

and can be neglected. According to equation (1.67) the NMR decay signal in the y-direction of the rotating frame can be obtained trough the trace:

$$S_y^{MAS}(t) = \frac{\mathbf{Tr}\left\{(\hat{\boldsymbol{I}}_y^i + \hat{\boldsymbol{I}}_y^j)\hat{\boldsymbol{\rho}}(t)\right\}}{\mathbf{Tr}\left\{(\hat{\boldsymbol{I}}_z^i + \hat{\boldsymbol{I}}_z^j)\hat{\boldsymbol{\rho}}(0)\right\}} = \cos\left[\int_0^t \omega_D^{ij}(t')\,dt'\right]. \tag{1.82}$$

To calculate the integral of the $\omega_D^{ij}(t)$ function defined by equation (1.80) it is convenient to neglect initial starting point of the rotor $\varphi_0 = 0$ (see equation (1.74)). Also coefficient $d_{q,0}(\vartheta_m)$ with $q = 0$ under MAS conditions vanish and equation (1.82) can be solved [Got95]

$$\begin{aligned}
S_y^{MAS}(t) &= \left\langle \cos\left\{\frac{3}{2}\frac{d_{ij}^{II}}{\omega_r}\Big[\sqrt{2}\sin(2\vartheta^{ij})\sin(\tfrac{1}{2}\omega_r t)\cos(\psi^{ij} + \tfrac{1}{2}\omega_r t)\right.\right. \\
&\qquad \left.\left. -\tfrac{1}{2}\sin^2(\vartheta^{ij})\sin(\omega_r t)\cos(2\psi^{ij} + \omega_r t)\Big]\right\}\right\rangle,
\end{aligned} \tag{1.83}$$

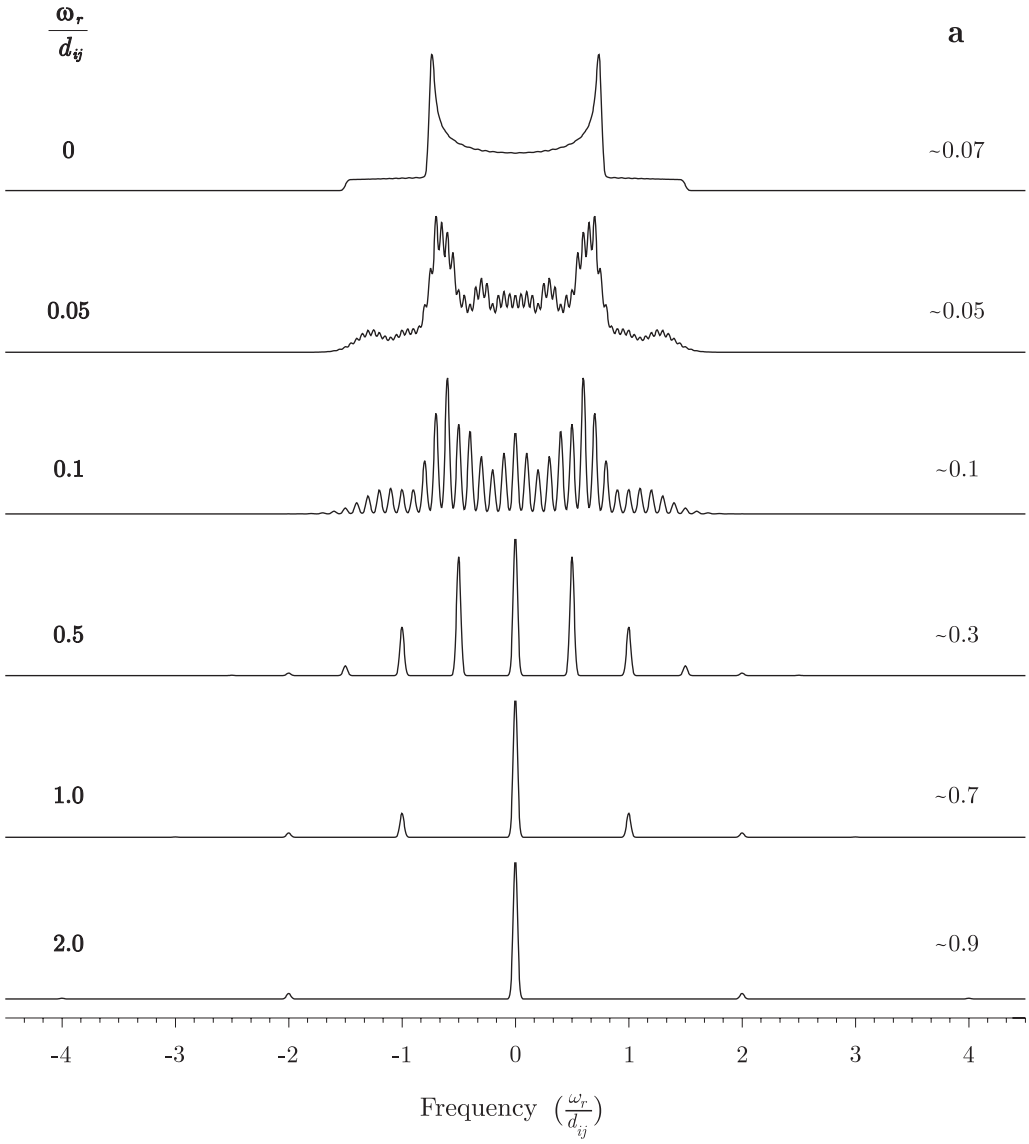

Figure 1.4: *Simulated spinning sideband pattern of single MAS experiment for different ratios between rotational frequency ω_r and dipole-dipole coupling d_{ij}^{II} ($\frac{\omega_r}{d_{ij}^{II}}$). Parameter* **a** *represents the amplitude of the highest point in each spectrum. Theoretical signal intensity (see equation (1.83)) is multiplied with Gaussian decay function to simulate more or less experimental FID.*

where $\langle \ldots \rangle$ means the powder averaging over the orientation of the dipolar coupled spin pairs. Analysing equation (1.83) it can be directly seen that for times $t = k \cdot \tau_r$ ($k \in \boldsymbol{N}$) the argument of the *cos* function vanish because $\sin(\frac{1}{2}\omega_r t) = 0$ as well as $\sin(\omega_r t) = 0$ so the signal becomes maximal for this time points. In addition intensity of the signal strongly depends on the orientation of the PAS to the rotor system. If PAS is oriented along the rotor axes i.e. $\vartheta_{ij} = 0$ signal will be constant and no rotor modulation can be

seen. For another orientation of the PAS system rotor modulation of the signal will be already preset. The Fourier transformation of equation (1.83) directly leads to the NMR spectrum with the sideband pattern. Simulated results[3] for powder sample are shown in Figure 1.4 for different ratios between rotational frequency ω_r and dipolar coupling d_{ij}^{II}. Static spectrum of dipolar coupled spin-½ pair ($\frac{\omega_r}{d_{ij}^{II}} = 0$ in the figure) is clearly split to the sideband pattern spectra with increasing spinning speed. At higher rotational frequencies ($\omega_r > 0.5\, d_{ij}^{II}$) central line already dominate the spectrum. Further increasing of ω_r leads to decreasing spinning sidebands as well as to increasing intensity of the central line as it is indicated in Figure 1.4. Experimental results from MAS experiment can be found in section 3.1.

1.7 Two-dimensional NMR spectroscopy

Up to now only one-dimensional (1D) spectroscopy has been considered where signal intensity is plotted only along one frequency axis. One r.f. pulse has been used to disturbs the spin system from its equilibrium. Just after that the system has been evolved under the influence of local interactions as FID (*free induction decay*), $S(t_2)$, during time t_2. Fourier transformation of $S(t_2)$ converts the time-domain signal into a frequency domain spectrum $S(\omega_2)$. In most of the cases in liquids as well as in solids the spectrum of desired sample is so complicated that lines of different nuclear species overlap and wished information can not be obtained. To overcome this difficulty a second time period, t_1, between preparation and detection periods can be included. During this period, called evolution period, nuclear motions may be different than during t_2 which can eventually influence the signal $S(t_2)$.

An intuitive scheme of two-dimensional (2D) experiment is shown in Figure 1.5. It consist of four periods in general: preparation, evolution, mixing and detection. Mixing period is not each time necessary ([Ern87, Rah86, Fre97]). The preparation period may be formed by a series of r.f. pulses to convert the system to the desired state. It can also consist of a delay long enough to allow the nuclei to reach equilibrium. During evolution time t_1 the system propagates under the influence of some internal Hamiltonians (see section 1.1). To manipulate the spin system after the evolution period the mixing period

[3]Home made computer program has been used for performing integrations over angles ϑ, ψ in equation (1.83).

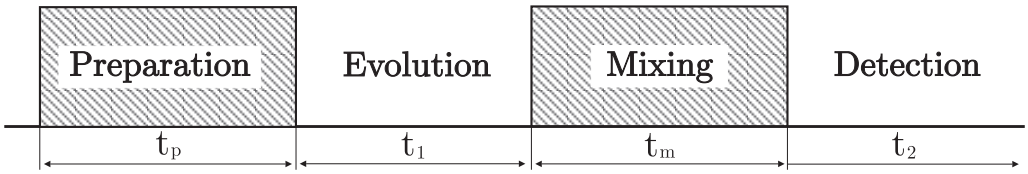

Figure 1.5: *Symbolic scheme for two-dimensional experiment.*

can be included (see e.g. [SR94]). In the last period a signal is detected for each increment of t_1 separately, thus a 2D free induction decay signal $S(t_1, t_2)$ is obtained. Double Fourier transformation of $S(t_1, t_2)$ will lead to the two-dimensional spectrum $S(\omega_1, \omega_2)$.

So far the relaxation of the time-domain signal has not been considered. Including it into FID artificial broadening of the spectrum lines is introduced. Fourier transformation (FT) of such a damping signal leads to the spectrum which can be written in terms of absorptive (A) and dispersive (D) components ([SR94]):

$$S(t_2) \quad \stackrel{\mathrm{FT}}{\longrightarrow} \quad S(\omega_2) = A(\omega_2) + i\, D(\omega_2) \tag{1.84}$$

In most of the cases only absorptive part $A(\omega_2)$ is interesting. It is positive definite and its integral does not vanish. Dispersive lineshape $D(\omega_2)$ exhibits antisymmetry and always consists of positive and negative intensities which superimposes in a complicated way. Thus, due to the antisymmetry, the integral over the dispersive lineshape vanishes. In addition dispersive signal has broader wings than the absorbtion component, resulting in a worse resolution.

In 2D spectroscopy it is often necessary to have purely absorptive spectrum $A(\omega_1)A(\omega_2)$, in short A_1A_2, in order to have optimum resolution and no spectral distortions. However, two successive Fourier transformations, over t_2 (FT_2) and t_1 (FT_1), from the 2D time-domain signal $S(t_1, t_2)$ give the spectrum

$$S(t_1, t_2) \quad \stackrel{\mathrm{FT}_1(\mathrm{FT}_2)}{\longrightarrow} \quad S(\omega_1, \omega_2) = (A_1A_2 - D_1D_2) + i\,(D_1A_2 - A_1D_2) \tag{1.85}$$

which contains a mixture of absorptive and dispersive parts. To obtain pure absorptive spectrum the data processing has to be modified (see [SR94] chapter 4, or [Ern87] chapter 6). It is often required to obtain real (cosine), S_c, and imaginary (sine), S_s, part of the time-domain signal according to t_1. This can be written shortly ([SR94])

$$\begin{aligned} S_c(t_1, t_2) &= \cos(\tilde{\omega}_1 t_1)\, e^{i\,\tilde{\omega}_2 t_2} \\ S_s(t_1, t_2) &= i\, \sin(\tilde{\omega}_1 t_1)\, e^{i\,\tilde{\omega}_2 t_2}\,, \end{aligned}$$

where $\tilde{\omega}_1$ and $\tilde{\omega}_2$ represent schematically all components present. Performing separately for both S_c and S_s Fourier transformation and setting dispersive part to zero, $D_2 = 0$, the real part of the spectrum corresponds to

$$Re\left[S_{c,s}(\omega_1, \omega_2)\right] = \tfrac{1}{2}\left(A(\omega_1 - \tilde{\omega}_1) \pm A(\omega_1 + \tilde{\omega}_1)\right) A_2\,. \tag{1.86}$$

Adding both $S_c(\omega_1, \omega_2)$ and $S_s(\omega_1, \omega_2)$ full absorption spectrum is obtained $A_1 A_2$. This technique is usually encountered in modern NMR instruments. It requires measuring of both $S_c(t_1, t_2)$ and $S_s(t_1, t_2)$ which together represent a *hypercomplex* dataset ([Ern87]). On the other hand an equivalent absorption spectrum can be obtained by TPPI (*time-proportional phase incrementation*) method of the sampling of the data. This method will be extensively used in this work. More details about TPPI used in the connection to a multiple quantum spectroscopy can be found in sections 2.4.3, 2.5.2 and 4.2.

2D spectroscopy covers a huge part of NMR. It can be intuitively divided in three categories: separation experiments, correlation experiments and exchange experiments. Basis overview of these experiments can be found in the excellent monographs [SR94] and [Ern87]. Besides this experimental techniques 2D spectroscopy enables also to study coherent transitions which do not contribute to the magnetization and can not be detected directly. This multiple quantum transitions/coherences can be detected indirectly during time t_1 with the help of 2D Fourier spectroscopy as will be seen in next chapters.